Development of a soft cable-driven hand exoskeleton for assisted rehabilitation training

Dawen Xu
College of Mechanical and Electrical Engineering, Nanjing University of Aeronautics and Astronautics, Jiangsu Province, China
Qingcong Wu
College of Mechanical and Electrical Engineering, Nanjing University of Aeronautics and Astronautics, Jiangsu Province, China and Jiangsu JWC Machinery CO., LTD, Jiangsu Province, China, and
Yanghui Zhu
College of Mechanical and Electrical Engineering, Nanjing University of Aeronautics and Astronautics, Jiangsu Province, China

Abstract

Purpose – Hand motor dysfunction has seriously reduced people's quality of life. The purpose of this paper is to solve this problem; different soft exoskeleton robots have been developed because of their good application prospects in assistance. In this paper, a new soft hand exoskeleton is designed to help people conduct rehabilitation training.

Design/methodology/approach – The proposed soft exoskeleton is an under-actuated cable-driven mechanism, which optimizes the force transmission path and many local structures. Specifically, the path of force transmission is optimized and cables are wound around cam-shaped spools to prevent cables lose during fingers movement. Besides, a pre-tightening system is presented to adjust the preload force of the cable-tube. Moreover, a passive brake mechanism is proposed to prevent the cables from falling off the spools when the remote side is relaxed.

Findings – Finally, three control strategies are proposed to assist in rehabilitation training. Results show that the average correlation coefficient of trajectory tracking is 90.99% and this exoskeleton could provide steady clamping force up to 35 N, which could meet the demands of activities in daily living. Surface electromyography (sEMG)-based intention recognition method is presented to complete assistance and experiments are conducted to prove the effectiveness of the assisted grasping method by monitoring muscle activation, finger angle and interactive force.

Research limitations/implications – However, the system should be further optimized in terms of hardware and control to reduce delays. In addition, more clinical trials should be conducted to evaluate the effect of the proposed rehabilitation strategies.

Social implications – May improve the ability of hemiplegic patients to live independently.

Originality/value – A novel under-actuated soft hand exoskeleton structure is proposed, and an sEMG-based auxiliary grasping control strategy is presented to help hemiplegic patients conduct rehabilitation training.

Keywords Rehabilitation training, Intention recognition, Soft hand exoskeleton, Transmission design, Under-actuated mechanism

Paper type Research paper

1. Introduction

The human hand is one of the most commonly used organs in people's daily life because it can interact with the external environment, and then assist people to finish many complex tasks. Many factors may cause hand functional limitations, such as various diseases (Wang *et al.*, 2019), increasing elderly population and repetitive and heavy works. To solve this problem, there has been growing interest in the research of exoskeleton technology to assist the motion of subjects with the motor disorder and rehabilitation troubles. Many researchers have been developing various exoskeleton to repair and enhance hand functions.

Existing hand rehabilitation systems could be mainly divided into two categories in terms of structural properties, namely, rigid exoskeleton robots (Tong *et al.*, 2011; Wege and Zimmermann, 2008) and soft exoskeleton robots (Popov *et al.*, 2016; Xiloyannis *et al.*, 2016; Lee *et al.*, 2014; Burns *et al.*, 2019). In these rigid robots, almost the movement of each finger needs to be driven by a motor, which not only increases the cost of the system but also complicates the control algorithm. Just as the paper (Tong *et al.*, 2011) showed, five linear actuators were mounted on the dorsal side to actuate a robotic hand, driving each finger to flex and extend. Another disadvantage of the rigid exoskeleton is that each rigid connecting rod needs to be highly matched with the joints of

The current issue and full text archive of this journal is available on Emerald Insight at: **https://www.emerald.com/insight/0143-991X.htm**

Industrial Robot: the international journal of robotics research and application

[ISSN 0143-991X]
[DOI 10.1108/IR-06-2020-0127]

National Natural Science Foundation of China. 51705240.
National Natural Science Foundation of Jiangsu x. BK20170783.
State Key Laboratory of Robotics and System (HIT) x. SKLRS-2018-KF-10.

Conflict of interest: We declare that we have no financial and personal relationships with other people or organizations that can inappropriately influence our work, there is no professional or other personal interest of any nature or kind in any product, service and/or company that could be construed as influencing the position presented in or the review of, the manuscript entitled, "Development of a soft cable-driven hand exoskeleton for assisted rehabilitation training."

Received 18 May 2020
Revised 17 July 2020
Accepted 28 July 2020

the human hand, otherwise it is very likely for the patient to suffer secondary injury and affect the user experience. Gears, rigid anchors and mechanical construction were integrated into the hand exoskeleton (Wege and Zimmermann, 2008), which certainly increased the risk of injury.

Soft exoskeleton robots have become increasingly popular because of their good characteristics such as flexible, relatively safe and lightweight, which makes up for the shortcomings of rigid ones. However, existing soft robots also have some deficiencies, such as excessive hand load, inaccurate transmission, too many hard anchor points and cumbersome control processes. A hand soft exoskeleton (Popov *et al.*, 2016) was developed for hand assistance. The hand was powered by four electric motors, which were all integrated into the forearm and then added to the burden on the hand. It not only increased the expenditure but also complicated the control process. For the cables-driven soft robotic glove (Xiloyannis *et al.*, 2016), when the hand flexed and extended at a constant rate, the cables were wound and released at a different rate. However, the spools driving the thumb, index and middle fingers were all round, which may make the cables lose and the transmission imprecise. In the paper (Lee *et al.*, 2014), a rehabilitation glove, which was also actuated by five motors and the forearm needed to bear the weight of the drive mechanism. What is worse, excessive hard anchors were added to the surface of the glove and then affected the users' experience. Besides, a rehabilitation glove called HEXOES (Burns *et al.*, 2019) was designed for hand rehabilitation, which was a soft cable-driven hand exoskeleton capable of independently actuating and sensing 10 degrees of freedom (DoF) of the hand. Flexion was driven by 10 filamentous nylon cables while the extension was passive and actuated by adjustable springs on the back of the hand, which made real-time continuous control a challenge.

Taking the advantages and disadvantages of existing exoskeleton robots into account, a new soft glove-type hand exoskeleton is proposed in this research. The exoskeleton optimizes the power transmission path and local structures. Specifically, the path of force transmission is optimized and the drive mechanism implements a pre-tightening system, cam-shaped spools and a passive brake mechanism, which ensures the reliability and accuracy of the transmission process. Characterization analysis shows that this exoskeleton has good performance in both motion and force control. The intention identification method which is based on logical muscle activation is proposed to conduct assisted training with the exoskeleton. The detailed designs of the exoskeleton are described in Section 2, followed by the performance in different controls in Section 3. Conclusions and future works in Section 4.

2. Design

Figure 1 gives an overview of this new exoskeleton system. This assistive system consists of three parts which are the drive unit, the transmission part and the glove itself. The design details of these parts will be described below.

2.1 Structure of the glove

The glove is the part that attaches cables to the body and transfers tension to the joints. After that, the glove makes contact with the object to complete the grasping. For the sake of comfort and safety, rigid mechanical connections are not desirable because they need to align well with human joints, otherwise they would cause secondary injury. In this research, the part in direct contact with the hand is designed based on a glove, which is soft and comfortable. The concept design of the glove is shown in Figure 2. Only three fingers (thumb, index and middle) are actuated based on their importance in executing most tasks of daily living. To measure the human-robot interaction force, three force-sensitive resistors (FSR) (Weikesi RP-C18.3-ST) are attached to the fingertip of these three fingers. Considering that the sensors are sensitive to the material of objects, rubber gaskets are laid on the surface of the sensors to improve contact conditions, which could obtain high-quality raw force signals. For aesthetics and protection, the surfaces of the FSRs are covered with insulating tapes. Furthermore, three flex sensors (Flex 2.2 and Flex 4.5) are integrated into the glove. Specifically, insulating tapes are used to firmly stick the calibrated three sensors to the dorsal side of the three fingers. Then, driven by the exoskeleton, each sensor adaptively flexes and measures the sum of the motion angles of the three joints [metacarpophalangeal point (MIP), proximal interphalangeal point (PIP) and distal interphalangeal point (DIP)]. The angle between the initial position and the final position is defined as the angle of finger movement, just as Figure 3 shows.

Figure 1 Prototype of a rehabilitation exoskeleton glove system

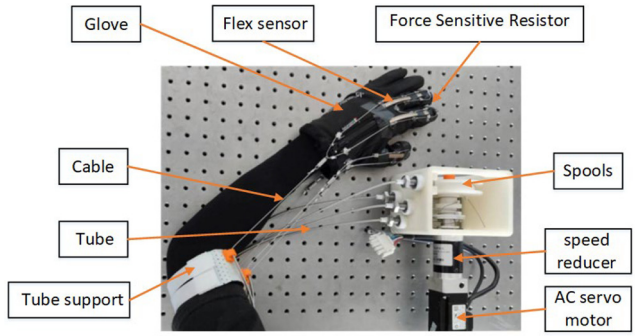

Figure 2 (A) and (B) are the palmar side and dorsal side of the glove, respectively (glove; tube; force-sensitive resistor (FSR); flex sensor; spools)

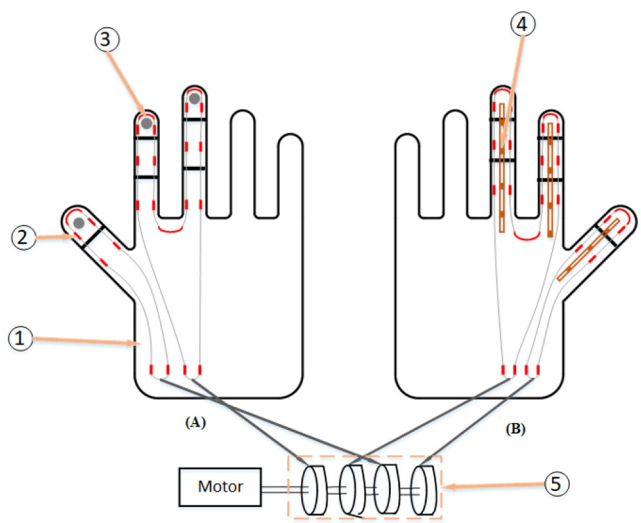

Figure 3 Angle measurement method. θ is the measured angle

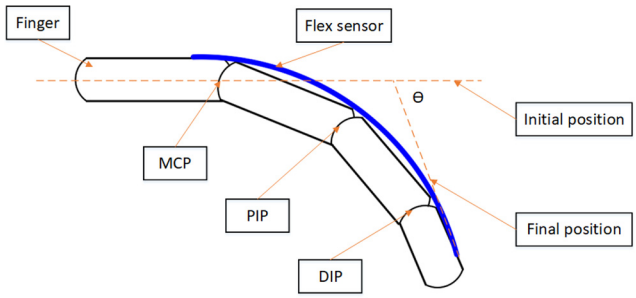

2.2 Transmission mechanism

In previous studies, differential mechanisms are often used for fingers under-actuation. When multiple fingers are under-driven, the human hand can adapt to not only two-dimensional but also three-dimensional (3D) curved surfaces (In *et al.*, 2017). In daily grasping activities, its not necessary to accurately control each joint (MIP, PIP and DIP) at the same time, but need to adapt the gloves to the shape of objects, ensuring the coupling relationships of each joint and realizing the rehabilitation training function in the grasping process. Therefore, a structure for the differential mechanism is proposed and the layout of cables is shown in Figure 2. To improve the stability of the anchor points and distribute the force between the fingers, tubes are installed on the joints of the thumb, index and middle fingers as the anchor points so that the cables can freely move through the tubes. As the cable has good rigidity and wears resistance, it guarantees the reliability of this system to a certain extent. Moreover, the tube is a kind of tubing spring, with a certain degree of elasticity and toughness. To ensure each joint of each finger to obtain the force transmitted by the cables, each small piece of tube is sewed at the predetermined position and then strong glue is used to glue the tube and the glove together. After that, the relative position of the tubes and glove would not change. Moreover, the diameter of the tubes has been chosen about twice the cable diameter to reduce the friction between the cables and tubes (Niestanak, 2017). A cable is used for the thumb to transfer force in each direction and one cable is used for index and middle finger, which not only takes advantage of the under-drive but also reduces the size and cost of the system. To improve the flexibility of movement, springs are connected to the cables mounted on the surface of the glove (Modeling and Training, 2018). Moreover, for the propose of obtaining transmitting force, tube support is installed in the forearm to support tubes. Once installed, it can not slide relative to the skin.

2.3 Drive unit

In this paper, a 3D-printed box-type actuator holder containing lots of mechanical components is placed away from the hand, which not only reduces the burden on the forearm but also solves the problem of insufficient installation space on the forearm. Details of the drive mechanism are shown in Figure 4. For the exoskeleton, it will be of great significance to select the befitting actuator and execution mode at first. Electric drive is selected as the driving mode because of its advantages, such as quieter, more durable and requires less maintenance. A high precision AC servo motor (YASKAWA SGM7J-01A7C6S) and a speed reducer with a speed reduction ratio of 1 to 20 are installed in the actuator. Moreover, the energy efficiency of a cable-driven system can be improved if it can maintain the actuation force while the remote side is relaxed (Ii *et al.*, 2013). Therefore, the passive brake mechanism is adopted, depicted in Figure 4 (b), which mainly consists of a one-way needle roller bearing, a 3D-printed rubber wheel, two guide rails and four needle bearings. The 3D-printed rubber wheel is made of a kind of rubber, which is elastic and hard to tear.

Passive braking systems have been analyzed in previous studies (In H., Jeong U. *et al.*, 2017). Also, experiments are designed to evaluate the function of our passive brake mechanism in this paper. Assuming that the rotating direction of the one-way bearing is fixed, so when the motor and one-way bearing rotate in the same or opposite direction, the cable is subject to sliding and rolling frictions, respectively, just as Figures 5(a) and 5(b) show. Three different diameter cables (0.6 mm, 0.8 mm and 1 mm) are selected in the experiment because both sliding friction and rolling friction are affected by pressures, and cables of different diameters would be subjected to different amounts of pressures in the brake mechanism. The tensions of the cables at both ends of the brake mechanism are measured by two tension sensors (JLBS-MD). The experimental layout is shown in Figure 6.

The motor is in speed mode and could output a constant speed. The following two equations could be obtained from Figure 5 and the experimental results are shown in Figures 7-8 and Table 1:

$$F_{sf} = F_2 - F_1 \tag{1}$$

$$F_{rf} = F_2 - F_1 \tag{2}$$

When the exoskeleton is working, the rolling friction in the target direction and the sliding friction in the opposite direction need to be overcome by the motor. If some factors cause the cable to

Figure 4 (a) The conceptual design of the driving mechanism (b) passive brake mechanism (c) pre-tightening system

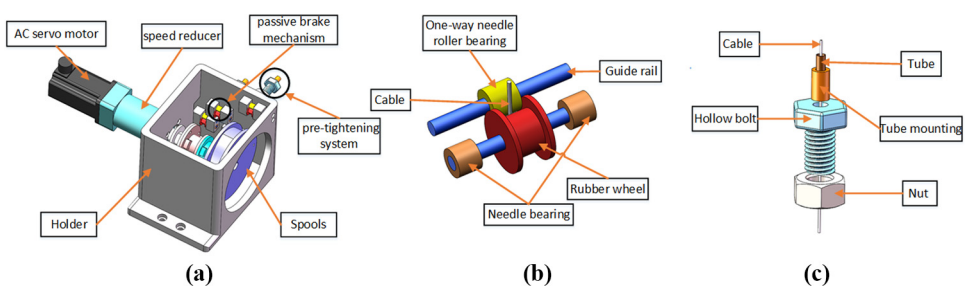

Figure 5 Friction between the cable and passive brake mechanism

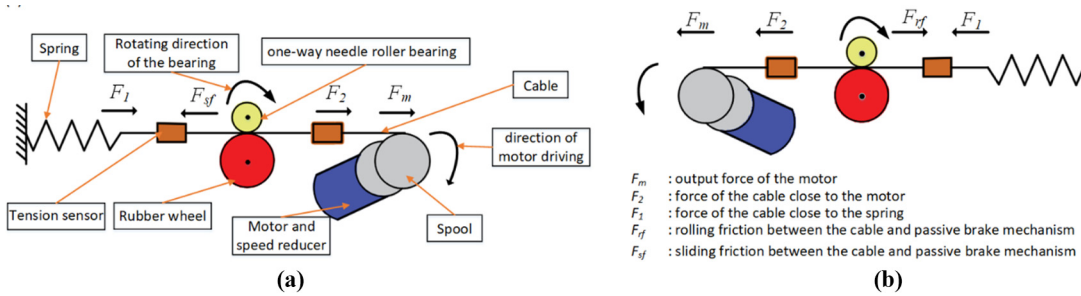

Notes: (a) Siding friction; (b) rolling friction

Figure 6 Experimental arrangement for evaluating the performance of a passive brake mechanism

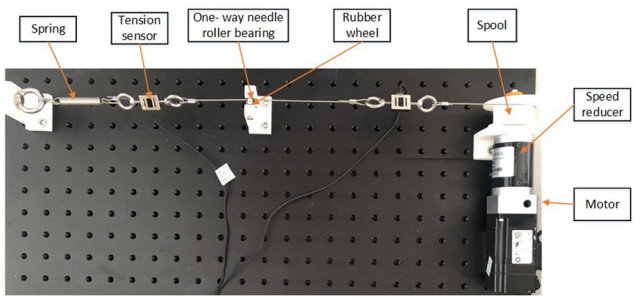

move when the remote side is relaxed, a certain amount of friction needs to be overcome, which could forbid the cable from slacking to some extent. Table 1 shows that when using different diameter cables in the experiments, the sliding and rolling frictions would fluctuate within a certain range, mainly due to the following two factors. One is that cables pass through a certain viscous rubber wheel at a relatively low speed, causing the friction to shake. The other is that the tension sensors and springs affect the pressure on the cable at the squeeze point during the movement.

Besides, if the selected cable is too thin or thick, it cannot play the role of passive braking or could consume more electrical energy. Therefore, cables with a diameter of 0.8 mm are selected to transmit force in this paper, playing the role of artificial tendons.

The pre-tightening system, shown in Figure 4(c), is composed of several components, mainly including a nut, a tube mounting and a hollow bolt. By adjusting the relative positions of the hollow bolt and the nut, the preload force of the tendon-tube can be adjusted, and thus the tendon is tensioned at the beginning. In this research, cables are wrapped around the spools and used to transfer force so it is necessary to keep them tensioned all the time. Hence, it is necessary to know how long the cables need to be wrapped when the finger flexes to its limit position. Experiments are designed to measure the changes in the length of the cables by two displacement sensors (GEERT HLC-200mm) during hand flexion. The three fingers are divided into two groups. One is the thumb and the other is the index and middle (I&M) fingers, which means a total of four cables are used to transmit the force during hand flexion and extension. To get general results, each group of fingers flex to its initial position three times at a certain speed, then the average of the four cables change lengths are shown in Figures 9-10.

Figure 7 Sliding frictions between the different diameters cables and passive brake mechanism during movement

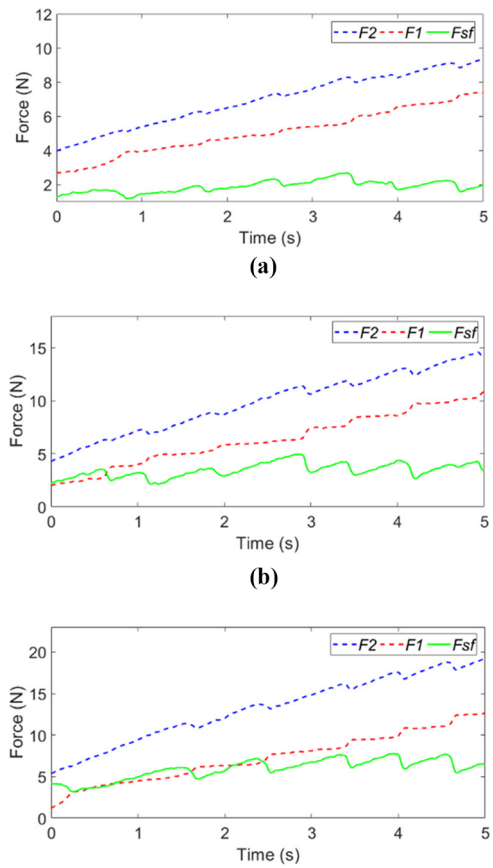

Notes: Notes: F_1: force of the cable close to the spring; F_2: force of the cable close to the motor; F_{sf}: sliding friction (a) 0.6 mm; (b) 0.8 mm; (c) 1.0 mm

During hand flexion, the length of the cables mounted on the palmar side and dorsal side of the glove would change. For the thumb, L_{tp} and L_{td} are the length changes of the cables laid on the palm side and dorsal side, respectively. For the I&M fingers, L_{imp} and L_{imd} are the length changes of the cables laid on the palm side and dorsal side, respectively. In this paper, the following

Figure 8 Rolling frictions between the different diameters cables and passive brake mechanism during movement

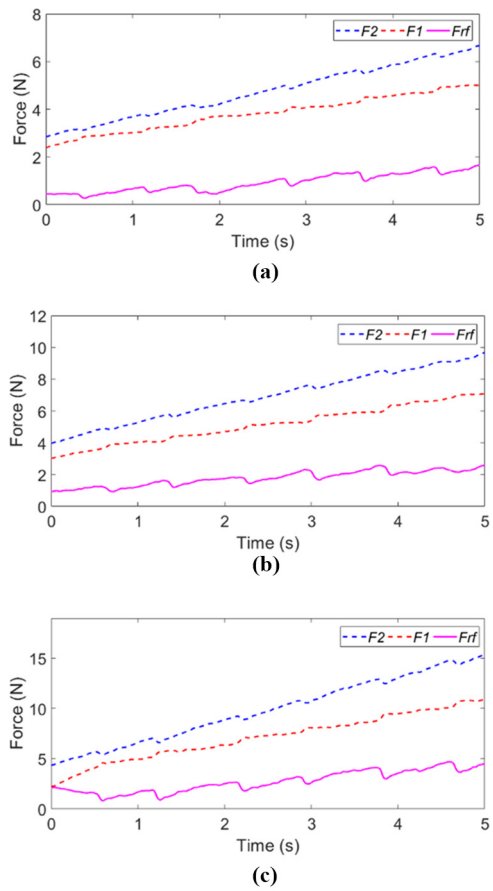

Notes: Notes: F_1: force of the cable close to the spring; F_2: force of the cable close to the motor; F_{rf}: rolling friction (a) 0.6 mm; (b) 0.8 mm; (c) 1.0 mm

Table 1 Sliding and rolling friction between the different diameters cables and passive brake mechanism during movement

Cable diameter	Sliding friction	Rolling friction
Cables		
0.6 mm	[1.2 N, 2.7 N]	[0.3 N, 1.6 N]
0.8 mm	[2.2 N, 5.0 N]	[1.0 N, 2.6 N]
1.0 mm	[3.2 N, 7.8 N]	[1.0 N, 4.7 N]

design has been made that the change length of the cables equals half the perimeter of a spool when the finger flexes to the limit position at a constant speed. In other words, the spools just rotate within 180° during the whole flexion. Two variables are used to represent the ratio relationships between the wrapped cable when the hand flexes, just as the following formulas describe:

$$f_t(\theta) = \frac{L_{td}}{L_{tp}} \tag{3}$$

$$f_{im}(\theta) = \frac{L_{imp}}{L_{imd}} \tag{4}$$

where θ is the rotation angle of the spools; $f_t(\theta)$ and $f_{im}(\theta)$ are the ratios between the cable length of the thumb and I&M fingers during hand flexion.

Figures 9(b) and 10(b) clearly show that for a certain group of fingers, the ratio of the wrapped cables mounted on the dorsal and palmar sides is not a constant, but varies with the rotation of the spools. Besides, four spools are driven by one motor. If two spools are all set circle-type for one group finger during hand flexion and extension, it will result in cables losing, inaccurate transmission, system response delay. Therefore, for one specific group, the cables should be wrapped around one circle-type spool and one cam-type spool. The following relationship existing between the circle-type spool and the cam-type spool can be expressed as equation (5):

$$S_2 = f_x(\theta_0) \cdot S_1 \tag{5}$$

where S_1 and S_2 are the lengths of the cables wrapped around the circle-type spool and the cam-type spool, just as Figure 11 shows. Besides, $f_x(\theta_0)$ represents that when the spools rotate θ_0, for the thumb, $f_x(\theta_0) = f_t(\theta_0)$; for the I&M fingers, $f_x(\theta_0) = f_{im}(\theta_0)$.

Based on the knowledge of mathematics, the following relationships can be established:

$$S_1 = \theta_0 \cdot R \tag{6}$$

$$S_2 = \int_0^{\theta_0} r(\theta) d(\theta) \tag{7}$$

Here, R is the radius of the circle-type spool; θ_0 represents the rotation angle of the spools. Besides, $r(\theta)$ is the radius of the curvature of the cam-type spool. Taking formulas equations (6) (7) into equation (5), such equation can be achieved:

Figure 9 (a) The wrapped cables length of the palmar and dorsal side during thumb flexion. (b) The ratio of the wrapped cables mounted on the dorsal and palmar side during thumb flexion

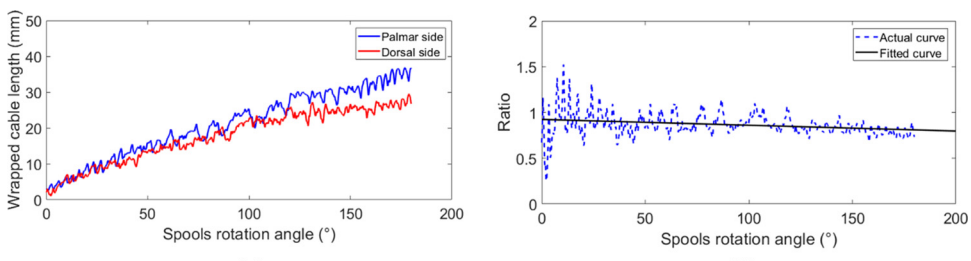

Figure 10 (a) The wrapped cables length of the palmar and dorsal side during I&M fingers flexion. (b) The ratio of the wrapped cables mounted on the palmar and dorsal side during I&M fingers flexion

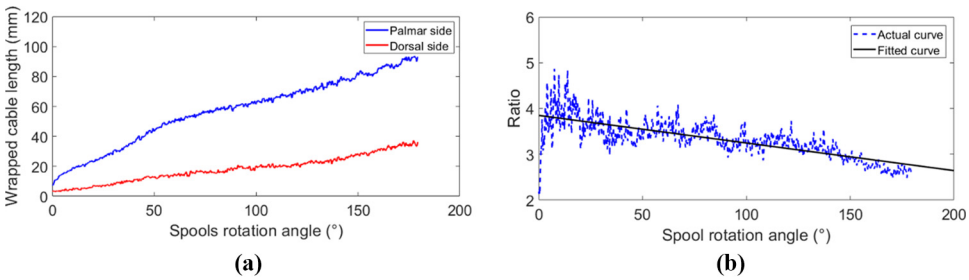

Figure 11 (a) and (b) are cables wrapping method of the circle-type spool and the cam-type spool for one group of fingers (thumb or index and middle), respectively

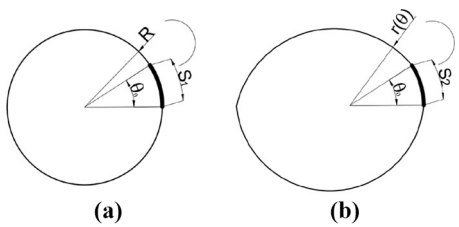

$$\int_0^{\theta_0} r(\theta)d(\theta) = \theta_0 \cdot R \cdot f_x(\theta_0) \tag{8}$$

Taking the derivative of θ_0 in equation (8):

$$r(\theta_0) = R \cdot [\theta_0 \cdot f_x(\theta_0)]' \tag{9}$$

The size of all the spools could be obtained from Figures 9(a), 10(a) and equation (9). The radiuses of the spools are shown in Table 2. The specific appearances of spools are shown in Figure 12. To reduce the overall weight of the device, all the spools are all 3D-printed from resin.

3. Glove control

To check the usability of this developed rehabilitation exoskeleton glove, characterization experiments have been conducted to test the performance of this device, including trajectory tracking and force control, surface electromyography (sEMG)-based assisted grasping control, which is shown in Figure 13 (Zhang *et al.*, 2019). In the early stage of rehabilitation pieces of training, patients have poor autonomous activities so passive pieces of training are the mainstay. In this case, the preset angle or interaction force is used as the input of the proportion-integral-derivative (PID) controller, and the signal of the angle sensor or the pressure sensor is used as the feedback signal to realize passive training. In the middle and later stages of rehabilitation pieces of training, patients have a certain degree of autonomy so auxiliary grasping could be conducted based on users' intention, and then achieve sports rehabilitation. Users could switch between these three training modes based on their needs. The performances and detailed experimental process will be discussed in the following three parts, respectively.

Table 2 The Radiuses of the spools (mm)

Finger name	Palmar side	Dorsal side
Thumb finger	11.46	$10.54 - 0.84\theta_0$
Index and middle finger	$43.56 - 4.88\theta_0$	12.10

Note: θ_0 (0-180°) represents the rotation angle of the spools

Figure 12 Four different sizes of spools driving the thumb, index and middle fingers

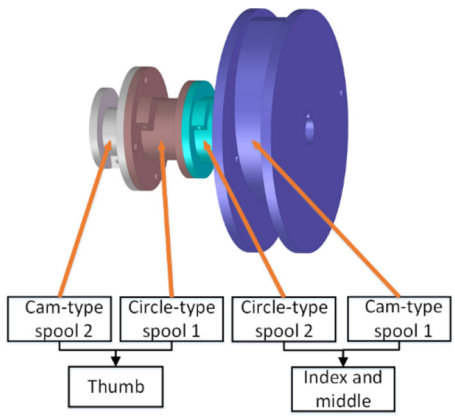

Figure 13 The overall control block diagram

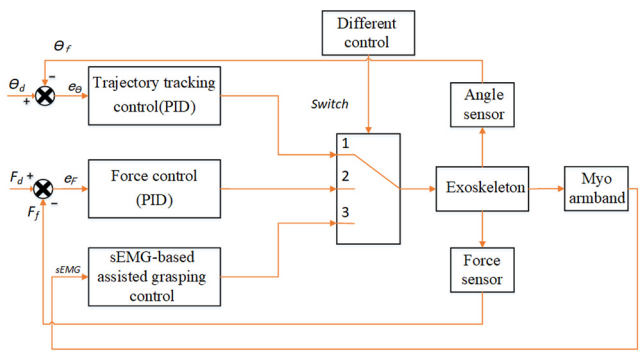

3.1 Trajectory tracking control

In the early stages of rehabilitation, patients mainly carry out passive training, which is completely driven by the exoskeleton. To this aim, it is necessary to control the bending angle of the fingers (Kazeminasab *et al.*, 2018), testing whether the fingers can reach the preset position quickly and accurately with the exoskeleton. In this research, trajectory tracking experiments of

the middle finger based on the PID controller are designed to evaluate the performance of this system in terms of rapidity and accuracy. The subject needs to follow the exoskeleton completely and stay relaxed in the experimental process.

The correlation coefficient is considered to quantitative analyze the efficacy of angle tracking, which could be described as follows:

$$\rho_{A_d,A_m} = \frac{Cov(A_d, A_m)}{\sigma_{A_d} \cdot \sigma_{A_m}} \tag{10}$$

where A_d and A_m represent the desired angle and measured angle, respectively; Cov defines the covariance. In addition, σ_{Ad} and σ_{Am} indicate the standard deviation of the desired and measured angles. Besides, to calculate the error between the actual joint torque and the estimated joint torque, root mean square error (RMSE) and normalized root mean square error (NRMSE) are taken into account (Lu *et al.*, 2019), which are shown as:

$$RMSE = \sqrt{\frac{\sum_{t=1}^{N}(A_{dt} - A_{mt})}{N}} \tag{11}$$

$$NRMSE = \frac{RMSE}{A_{mt\max} - A_{mt\min}} \tag{12}$$

where N is the number of angle signals; A_{dt}, A_{mt} is the desired and measured angle at time t. A_{mtmax}, A_{mtmax} represent the maximum and minimum of A_{mt}.

Table 3 Results of the trajectory tracking control experiment

Curve type	ρ (%)	*RMSE* (deg)	*NRMSE* (%)
Sine curve	85.41	8.93	19.84
Custom trapezoid curve	96.57	4.44	11.1

Results of the trajectory tracking control experiment are shown in Table 3 and Figure 14, which show that desired and measured signals have relatively good correlations. The errors between the actual and desired angle are shown in (c) and (d), which range from −19° to 13° and mainly come from the easy deformation of the glove and the presence of springs, but it is within the allowable range.

3.2 Force control

It is not enough to control the bending angle of fingers in the process of human-computer interaction. Force control could ensure user safety during rehabilitation training and prevent objects from being destroyed, so it is indispensable to check if the device could provide a stable desired clamping force. To demonstrate the capability of this exoskeleton in providing forces for the hand in interaction with objects, the force exerted by the glove on the aluminum box is examined by experiments based on the PID controller in this part. Pre-set expected contact force and the sum of fingertip force measured by the three sensors is selected as the input and feedback signal of the controller. The experimenter grasps the aluminum box with the help of the glove, while exerting no force of his own, just as shown in Figure 15.

The results of the force control for several desired forces are shown in Figure 16. The exoskeleton needs to provide a certain range of clamping force when the experimenter is carrying out assisted grasping. Therefore, target clamping forces are set from 5 to 35 N according to the actual capacity of normal users. Besides, the desired forces are set as some constants, there is no need to consider the issue of tracking accuracy. Then, from the perspective of safety and success rate, the proportional parameter in the PID controller is deliberately adjusted to be small, so it took a long time to reach the target force. Results display that the interaction force can reach the preset force and remain stable after a few seconds of movement, which proves the exoskeleton could provide stable clamping force up to 35 N.

Figure 14 The results of middle finger trajectory tracking experiments

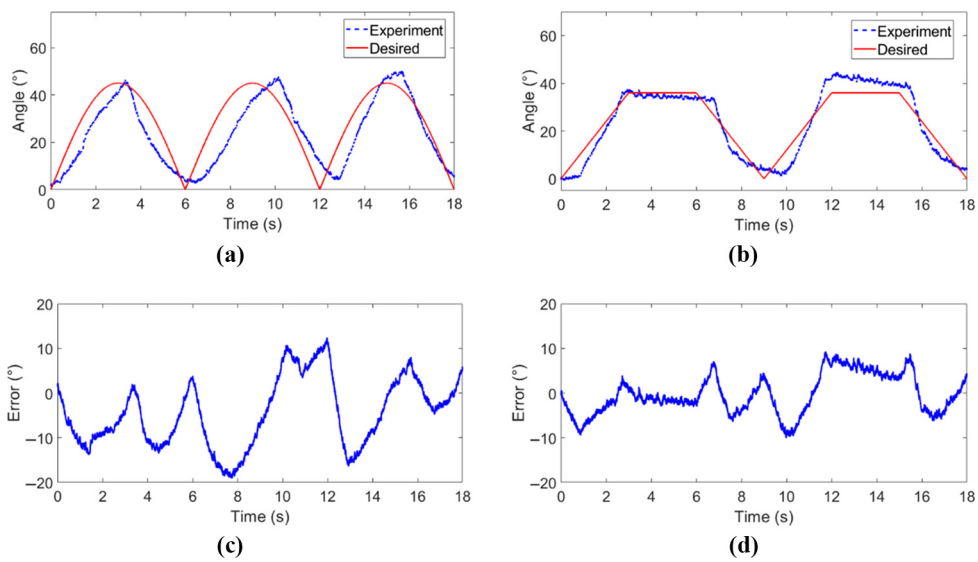

Notes: (a) (c) The target trajectory is a sine curve; (b) (d) The target trajectory is a custom trapezoid curve

3.3 Surface electromyography -based assisted grasping control strategy

To realize the human-computer interaction in rehabilitation training, the biggest challenge is to accurately identify the user's motion intention in a rapid and accurate way. Recognition of human motion intention based on biological signals has become increasingly popular because of its promising prospect in human-computer interaction. Moreover, sEMG is widely used in the robotic systems to obtain human motion intention due to its effectiveness, safety, portability and non-invasive, non-delay features (Li *et al.*, 2014). Therefore, an sEMG-based assisted grasping control strategy is proposed to conduct training.

Myo armband is used to collect the sEMG signals of muscles because it can pick up relatively weak signals and complete signal amplification and feature extraction. Myo armband has eight electrodes, but only two electrodes are used to collect the signals of the related muscles on the forearm. Moreover, the collected sEMG signals are values ranging from −128 to 128. When the sEMG signals have been collected, they must first go through a series of processing, which includes different filtering operations and other processing methods (Lu *et al.*, 2019) to reduce the effect of noise and complete the transition from the original sEMG to muscle activation. The specific operations are shown in Figure 17. Specifically, a 10-500 Hz second-order Butterworth band-pass filter is used to filter low-frequency interference caused by electrode and muscle movement, and a 50 Hz notch filter is used to filter 50 Hz power frequency disturbance. Furthermore, the muscle activation envelope could be obtained through the full-wave rectifier and 1 Hz first-order Butterworth low-pass filter. On the premise of ensuring high-quality signals, the number of filter iterations is reduced and the appropriate cut-off frequency is chosen to reduce the signal delay.

The focus of the control strategy is to recognize motion intention. Users' motion intents can be divided into three

Figure 15 Force control experiment setup

Figure 16 The results for the thumb and I&M fingers fingertip's force control

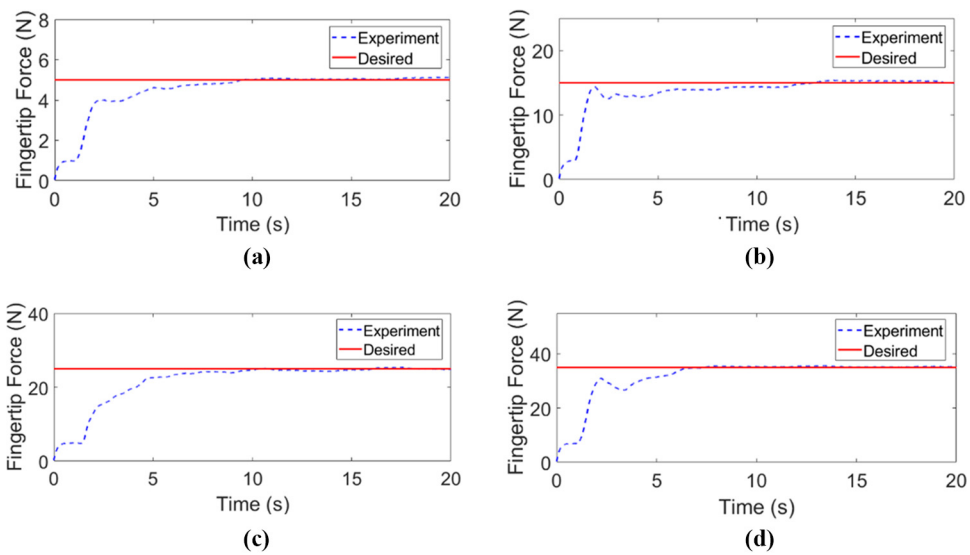

Notes: (a) Desired fingertip force = 5 N, (b) desired fingertip force = 15 N; (c) desired fingertip force = 25 N; (d) desired fingertip force = 35 N

Figure 17 sEMG signals processing steps to obtain muscle activation

Figure 18 Flowchart for detecting users' intention with sEMG signals extract from EDC and FDS muscles

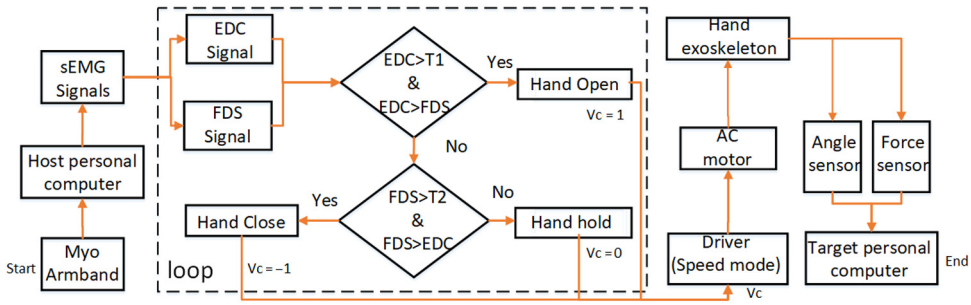

categories, namely, hand open, hand hold and hand close. The hand motion is closely related to the two muscles of the forearm (Cao and Zhang, 2016), namely, extensor digitorum communis (EDC) muscle and flexor digitorum superficialis (FDS) muscle. EDC muscle is used to detect hand open intent and FDS muscle is used to detect hand close intent. The sequences of the control experiment are shown in Figure 18. The thresholds of EDC and FDS activation are set through experiments.

In the current study, four healthy subjects, 23-51 years of age, height 160-181 cm, weight 49-79 kg, two women and two men, had been involved in the experiments and provided informed consent. The implemented experimental approaches of this research have been approved by the Institutional Review Board of Nanjing University of Aeronautics and Astronautics. Experiments are designed to verify the feasibility of this control strategy and the results are shown in Figure 19. The experimenter slowly grabs an aluminum box with the exoskeleton after correctly identifying the motion intents. When the user's intention is judged as hand close, the motor rotates in a forward direction (Vc = 1). Besides, the angle of the middle finger gradually increases and the contact force begins to increase as the hand touches the box slowly. When the user's intention is judged as hand hold, the rotating speed of the motor is zero (Vc = 0). Moreover, the angle of the middle finger and contact force is basically unchanged. When the user's intention is judged as hand open, the motor rotates inversely (Vc = −1). The angle of the middle finger and the contact force gradually decrease. Results demonstrate that the exoskeleton could help users to carry out rehabilitation training based on intention recognition.

4. Conclusion and future works

In this research, an under-driven soft exoskeleton glove was developed to help patients with assisted grabbing. Design details were proposed to meet the usage requirements, optimize the force transmission path and local structures. Trajectory tracking and force control experiments were designed to verify the glove's performance in recording motion information. Results showed that the average correlation coefficient between the desired and measured angle is 90.99%. Also, the glove could provide a stable clamping force of 35 N, which was enough for activity of daily livings. Besides, an sEMG-based control strategy was proposed to conduct assisted rehabilitation training. Users' intents could be monitored by Myo armband and established connections with sEMG. Grasping experimental results showed that this strategy could identify the person's motion intention effectively and enable

Figure 19 The experimenter grabs, holds and releases an aluminum box with the soft mechanical glove

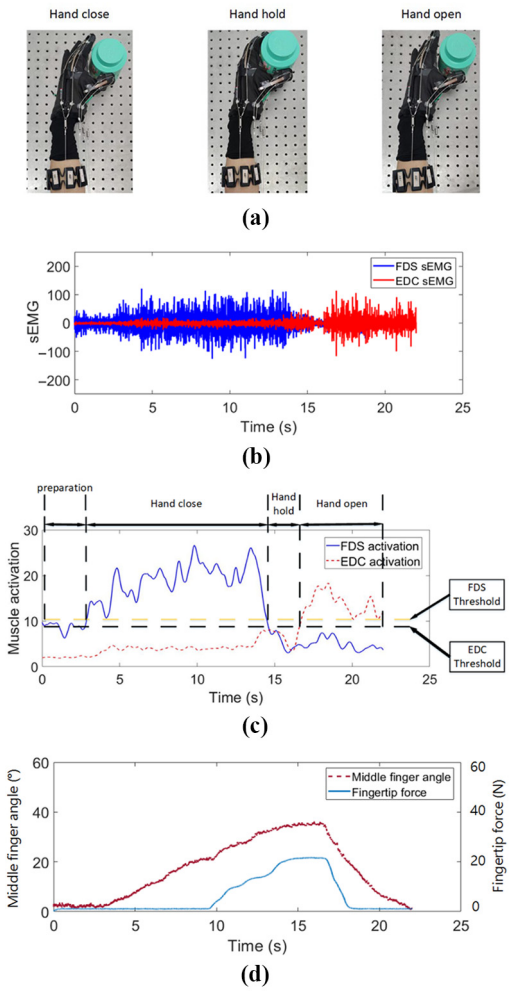

Notes: (a) State of the hand; (b) sEMG signals of EDC and FDS muscles. The sEMG signals collected by the Myo armband are values ranging from −128 to 128; (c) Muscle activation and its thresholds during a different state of the hand. To distinguish the sEMG signals of FDS and EDC muscles, the filtered muscle activations need to be multiplied by the corresponding coefficients; (d) Middle finger angle and sum of fingertip force of thumb, index and middle finger

users to complete the grasping action with the assistance of the exoskeleton.

Rehabilitation training is generally carried out in three steps, which are identifying the user's movement intentions, proposing real-time accurate control strategies and evaluating the effectiveness of rehabilitation. The first two steps have been introduced in detail, so establishing an evaluation system to evaluate the effectiveness of rehabilitation training would be the focus of the future works. Besides, many patients with hand disorders will be recruited in our rehabilitation training.

References

Burns, M.K., Member, G.S., Pei, D. and Member, S. (2019), "Myoelectric control of a soft hand exoskeleton using kinematic synergies", *IEEE Transactions on Biomedical Circuits and Systems*, Vol. 13 No. 6, pp. 1351-1361.

Cao, H. and Zhang, D. (2016), "Soft robotic glove with integrated sEMG sensing for disabled people with hand paralysis", *2016 IEEE International Conference on Robotics and Biomimetics, ROBIO 2016*, pp. 714-718.

Ii, M.A.D., Fischer, S.A., Gauthier, P.W., Luna, C.H.M., Clancy, E.A. and Fischer, G.S. (2013), "A soft robotic exomusculature glove with integrated sEMG sensing for hand rehabilitation", *2013 IEEE 13th International Conference on Rehabilitation Robotics (ICORR)*, pp. 1-7.

In, H., Cho, K., Kim, K. and Lee, B. (2011), "Jointless structure and under-actuation mechanism for compact hand exoskeleton", *2011 IEEE International Conference on Rehabilitation Robotics*, No. 2010, pp. 1-6.

In, H., Jeong, U., Lee, H. and Cho, K.J. (2017), "A novel Slack-Enabling tendon drive that improves efficiency, size, and safety in soft wearable robots", *IEEE/ASME Transactions on Mechatronics*, Vol. 22 No. 1, pp. 59-70.

Kazeminasab, S., Hadi, A., Alipour, K. and Elahinia, M. (2018), "A rehabilitation gait for the balance of human and lower extremity exoskeleton system based on the transfer of gravity center", *Industrial Robot: The International Journal of Robotics Research and Application*, Vol. 45 No. 5, pp. 623-633.

Lee, S.W., Landers, K.A. and Park, H. (2014), "Development of a biomimetic hand exotendon device (BiomHED) for restoration of functional hand movement Post-Stroke", *IEEE Transactions on Neural Systems and Rehabilitation*, Vol. 22 No. 4, pp. 886-898.

Li, Z., Wang, B., Sun, F., Yang, C., Xie, Q. and Zhang, W. (2014), "SEMG-based joint force control for an upper-limb power-assist exoskeleton robot", *IEEE Journal of Biomedical and Health Informatics*, Vol. 18 No. 3, pp. 1043-1050.

Lu, L., Wu, Q., Chen, X., Shao, Z., Chen, B. and Wu, H. (2019), "Development of a sEMG-based torque estimation control strategy for a soft elbow exoskeleton", *Robotics and Autonomous Systems*, Vol. 111, pp. 88-98.

Modeling, D. and Training, R. (2018), "Development, dynamic modeling, and multi-modal control of a therapeutic exoskeleton for upper limb rehabilitation training".

Niestanak, V.D. (2017), "A new underactuated mechanism of hand tendon injury rehabilitation", *2017 5th RSI International Conference on Robotics and Mechatronics (ICRoM)*, No. IcRoM, pp. 400-405.

Popov, D., Gaponov, I. and Ryu, J. (2016), "Portable exoskeleton glove with soft structure for hand assistance in activities of daily living", *IEEE/ASME Transactions on Mechatronics*, Vol. 4435, pp. 1-11.

Tong, K.Y., Hu, X.L., Fung, K.L., Wei, X.J., Rong, W. and Susanto, E.A. (2011), "An EMG-driven exoskeleton hand robotic training device on chronic stroke subjects task training system for stroke rehabilitation", *2011 IEEE International Conference on Rehabilitation Robotics*.

Wang, H., Yang, C., Yang, W., Deng, M., Ma, Z. and Wei, Q. (2019), "A rehabilitation gait for the balance of human and lower extremity exoskeleton system based on the transfer of gravity center", *Industrial Robot: The International Journal of Robotics Research and Application*, Vol. 46 No. 5, pp. 608-621.

Wege, A. and Zimmermann, A. (2008), "Electromyography sensor based control for a hand exoskeleton", *2007 IEEE International Conference on Robotics and Biomimetics (ROBIO)*, pp. 1470-1475.

Xiloyannis, M., Cappello, L., Khanh, D.B., Yen, S. and Masia, L. (2016), "Modelling and design of a synergy-based actuator for a tendon-driven soft robotic glove", *2016 6th IEEE International Conference on Biomedical Robotics and Biomechatronics (BioRob)*, pp. 1213-1219.

Zhang, F., Lin, L., Yang, L. and Fu, Y. (2019), "Design of an active and passive control system of hand exoskeleton for rehabilitation", *Applied Sciences (Switzerland)*, Vol. 9 No. 11.

About the authors

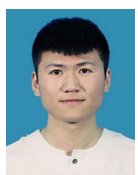

Dawen Xu received the BS degree in mechatronics engineering from Suzhou University, Suzhou, China, in 2018. He is currently pursuing an MS degree in mechatronics engineering with the College of Mechanical and Electrical Engineering, Nanjing University of Aeronautics and Astronautics, Nanjing, China. His research interests include rehabilitation robot, human-robot interaction control, Intention recognition and soft exoskeletons.

Qingcong Wu received the BS and PhD degrees in mechatronics engineering from Southeast University, Nanjing, China, in 2011 and 2016, respectively. He is currently an assistant professor with the College of Mechanical and Electrical Engineering, Nanjing University of Aeronautics and Astronautics, Nanjing, China. His major research interests include robotics, nonlinear control, tendon-sheath transmission theory, gravity balancing theory and the application of exoskeleton to neuromuscular rehabilitation. Qingcong Wu is the corresponding author and can be contacted at: wuqc@nuaa.edu.cn

Yanghui Zhu received a BS degree from Nanjing University of Aeronautics and Astronautics, Nanjing, China, in 2017. Currently, he is working toward an MS degree in the College of Mechanical and Electrical Engineering at Nanjing University of Aeronautics and Astronautics. His major research interests include exoskeleton robot, robot kinematics, Variable stiffness control and inverse kinematics.